

Ba₂AlSi₅N₉—A New Host Lattice for Eu²⁺-Doped Luminescent Materials Comprising a Nitridoalumosilicate Framework with Corner- and Edge-Sharing Tetrahedra

Juliane A. Kechele,[†] Cora Hecht,[†] Oliver Oeckler,[†] Jörn Schmedt auf der Günne,[†]
Peter J. Schmidt,[‡] and Wolfgang Schnick^{*,†}

Department Chemie und Biochemie, Ludwig-Maximilians-Universität München, Butenandtstrasse 5-13 (D),
D-81377 München, Germany, and Philips Technologie GmbH, Forschungslaboratorien, Solid State
Lighting, Weisshausstrasse 2, D-52066 Aachen, Germany

Received December 1, 2008. Revised Manuscript Received February 2, 2009

Ba₂AlSi₅N₉ was synthesized starting from Si₃N₄, AlN, and Ba in a radio-frequency furnace at temperatures of about 1725 °C. The new nitridoalumosilicate crystallizes in the triclinic space group *P*1 (no. 1), *a* = 9.860(1) Å, *b* = 10.320(1) Å, *c* = 10.346(1) Å, α = 90.37(2)°, β = 118.43(2)°, γ = 103.69(2)°, *Z* = 4, *R*1 = 0.0314. All synthesized crystals were characteristically twinned by reticular pseudomerohedry with twin law (1 0 0, −0.5 −1 0, −1 0 −1). The crystal structure of Ba₂AlSi₅N₉ was determined from single-crystal X-ray diffraction data of a twinned crystal and confirmed by Rietveld refinement both on X-ray and on neutron powder diffraction data. Statistical distribution Si/Al is corroborated by lattice energy calculations (MAPLE). ²⁹Si and ²⁷Al solid-state NMR are in accordance with the crystallographic results. Ba₂AlSi₅N₉ represents a new type of network structure made up of TN₄ tetrahedra (T = Si, Al). Highly condensed layers of dreier rings with nitrogen connecting three neighboring tetrahedral centers occur which are further crosslinked by dreier rings and vierer rings. The dreier rings consist of corner-sharing tetrahedra, whereas some of the vierer rings exhibit two pairs of edge-sharing tetrahedra. In the resulting voids of the network there are eight different Ba²⁺ sites with coordination numbers between 6 and 10. Thermogravimetric investigations confirmed a thermal stability of Ba₂AlSi₅N₉ up to about 1515 °C (He atmosphere). Luminescence measurements on Ba₂AlSi₅N₉:Eu²⁺ (2 mol % Eu²⁺) with an excitation wavelength of 450 nm revealed a broadband emission peaking at 584 nm (FWHM = 100 nm) originating from dipole-allowed 4f⁶(⁷F)5d¹ → 4f⁷(⁸S_{7/2}) transitions.

Introduction

In past years, (oxo)nitridosilicates and oxonitridoalumosilicates have received remarkable attention in materials science, because these thermally and chemically rather stable compounds exhibit particularly promising optical properties as well. A number of (oxo)nitridosilicates (e.g., M₂Si₅N₈ (M = Ca, Sr, Ba), MSi₂O₂N₂ (M = Ca, Sr, Ba)) are suited as host lattices for highly efficient rare-earth doped luminescent materials applied in phosphor-converted (pc-) light-emitting diodes (LEDs).^{1–6}

Oxonitridosilicates represent an intermediate class of compounds between classical oxosilicates and nitridosili-

cates.⁷ The latter can be formally derived from oxosilicates by an exchange O/N, yielding SiN₄ tetrahedra. However, this substitution gives rise to a manifold of additional structural possibilities. While oxygen in classical oxosilicates usually occurs in terminal O^[1] or simply bridging O^[2] function, nitrogen can additionally act as a triply (N^[3]) or even quadruply (N^[4]) bridging atom. Consequently, nitridosilicates exhibit a more variable degree of condensation in the range 1:4 ≤ κ ≤ 3:4 (i.e., the molar ratio Si:(N,O)) as compared with classical oxosilicates (1:4 ≤ κ ≤ 1:2).^{7,8} Furthermore, SiN₄ tetrahedra can share both common corners and edges while edge-sharing of SiO₄ tetrahedra has only been postulated for fibrous SiO₂,⁹ which was assumed to be isostructural with SiS₂. However, the existence and true nature of this unique silica polymorph has not been unequivocally confirmed as yet.

Edge-sharing of SiN₄ tetrahedra has only been observed in a few cases. Its relative stability is a consequence of the better polarizability of nitride anions compared to oxide

* To whom correspondence should be addressed. Fax: (+49)89-2180-77440. E-mail: wolfgang.schnick@uni-muenchen.de.

[†] Ludwig-Maximilians-Universität München.

[‡] Philips Technologie GmbH.

(1) Mueller-Mach, R.; Mueller, G.; Krames, M. R.; Höpfe, H. A.; Stadler, F.; Schnick, W.; Juestel, T.; Schmidt, P. *Phys. Status Solidi A* **2005**, *202*, 1727.

(2) Xie, R.-J.; Hirotsaki, N. *Sci. Technol. Adv. Mater.* **2007**, *8*, 588.

(3) Xie, R.-J.; Hirotsaki, N.; Kimura, N.; Sakuma, K.; Mitomo, M. *Appl. Phys. Lett.* **2007**, *90*, 191101/1.

(4) Piao, X.; Horikawa, T.; Hanzawa, H.; Machida, K. *Appl. Phys. Lett.* **2006**, *88*, 161908.

(5) Li, Y. Q.; deWith, G.; Hintzen, H. T. *J. Solid State Chem.* **2008**, *181*, 515.

(6) Kimura, N.; Sakuma, K.; Hirafune, S.; Asano, K.; Hirotsaki, N.; Xie, R.-J. *Appl. Phys. Lett.* **2007**, *90*, 051109/1.

(7) Schnick, W.; Huppertz, H. *Chem. Eur. J.* **1997**, *3*, 679.

(8) Schnick, W.; Schlieper, T.; Huppertz, H.; Köllisch, K.; Orth, M.; Bettenhausen, R.; Schwarze, B.; Lauterbach, R. *Phosphorus, Sulfur Silicon Relat. Elem.* **1997**, *124/125*, 163.

(9) Weiss, A.; Weiss, A. *Z. Anorg. Allg. Chem.* **1954**, *276*, 95.

anions and was observed in compounds like MSiN₂ (M = Ba, Sr),¹⁰ BaSi₇N₁₀,¹¹ and Ba₅Si₂N₆.¹²

Contrary to the (oxo)-nitridosilicates and oxonitridoalumosilicates the class of nitridoalumosilicates, which represents an intermediate between nitridosilicates and nitridoaluminates, is comparatively unexplored so far. The knowledge of nitridoalumosilicates is limited. No mineral is known in the system M–Si–Al–N, and only a few compounds have been synthesized and characterized. To the best of our knowledge, MSiAlN₃ (M = Be, Mg, Mn, Ca, Sr),^{13–15} Ca₅Si₂Al₂N₈,^{13,16} Ca₄SiAl₃N₇,^{13,16} filled α-Si₃N₄-type compounds,¹⁷ La₁₇Si₉Al₄N₃₃,¹⁸ Li_xAl_{12–3x}Si_{2x}N₁₂ (1 ≤ x ≤ 3),¹⁹ and SrAlSi₄N₇^{20,21} are the only compounds of this class observed so far. Some of these compounds have particularly promising properties similar to those of nitridosilicates. In this context, several investigations of the luminescence properties of Eu²⁺-doped CaSiAlN₃ have been carried out and showed specifically promising luminescence properties so that this material has emerged as an important red phosphor for white light pc-LEDs.^{22–25}

In this contribution, we report the synthesis, crystal structure, and properties of the nitridoalumosilicate Ba₂AlSi₅N₉, which contains a novel, unusual silicate framework with corner- and edge-sharing tetrahedra.

Experimental Section

Synthesis. For the synthesis of Ba₂AlSi₅N₉, 1.0 mmol (41.5 mg) of AlN (Tokuyama, Tokyo, 99 %), 0.7 mmol (95.3 mg) of Si₃N₄ (Ube Industries Ltd., Tokyo, 98%), and 0.8 mmol (113.4 mg) of Ba (A.B.C.R., 99.9 %) as small pieces were mixed in an agate mortar and filled into a tungsten crucible under argon atmosphere in a glove box (Unilab, MBraun; O₂ < 1 ppm, H₂O < 1 ppm). For the Eu doped samples 2% of the Ba amount was substituted by Eu (A.B.C.R., 99.9 %) as small pieces.

Under purified N₂, the crucible was heated to 800 °C with a rate of about 78 °C min⁻¹ in the reactor of a radio-frequency furnace²⁶ before the temperature was increased to 1725 °C during 2 h. This maximum temperature was kept for 5 h. Subsequently, the crucible

was cooled down to 1300 °C with a rate of about 85 °C h⁻¹ before quenching to room temperature by switching off the furnace. The samples contain Ba₂AlSi₅N₉ as colorless, air- and water-resistant crystals and microcrystalline by-products such as Ba₂Si₅N₈²⁷ or BaSi₇N₁₀.¹¹ These impurities could be removed by flotation with isopropyl alcohol.

Elemental analyses on selected crystals were performed by energy dispersive X-ray spectroscopy (EDX) using a JSM-6500F scanning electron microscope (Jeol) with a Si/Li EDX detector (Oxford Instruments, model 7418). The determined composition is in accordance with the structure model within the typical error ranges (calcd Ba₂AlSi₅N₉ (in wt%) Ba 48, Al 5, Si 25, N 22; found (in wt %) Ba 48, Al 4, Si 22, N 26). The nitrogen and oxygen contents were determined by EELS measurements carried out with a Gatan Tridien 863 P spectrometer attached to TEM Titan 80-300 (FEI Company, OR, USA). Only marginal amounts of oxygen could be detected, which might be explained either by small amounts of oxygen incorporated in the structure or by slight surface contamination. The results of the EDX and EELS measurements were confirmed by an elemental analysis (double determination, Mikroanalytisches Labor Pascher, Remagen, Germany). A sample doped with Eu (2%) was used for this analysis. The analysis is in accordance with the structure model within the typical error ranges (calcd Ba₂AlSi₅N₉ (in wt %) Ba 47.8, Al 4.7, Si 24.7, N 22.2, Eu 0.5; found (in wt%) Ba 47.6, Al 5.6, Si 24.3, N 20.6, O 0.7, Eu 0.5). The oxygen content determined is close to the detection limit; however, as the charge balance can easily be adjusted by the Si:Al ratio, minute amounts of oxygen can hardly be completely excluded in nitridoalumosilicates.

Single-Crystal X-ray Analysis. Single crystals of Ba₂AlSi₅N₉ were isolated and initially examined by Laue photographs recorded on a Buerger camera equipped with an image plate system (Fuji BAS-1800). Single-crystal X-ray data were collected on a STOE IPDS I diffractometer (Stoe & Cie., Darmstadt) with Mo Kα radiation (0.71073 Å, graphite monochromator). All investigated crystals were characteristically twinned by reticular pseudomerohedry. The structure was solved by direct methods from data belonging to one domain orientation only. In the refinement, all reflections from both domain orientations were used, taking into account the twin law (1 0 0, -0.5 -1 0, -1 0 -1). The SHELX suite of programs was used for all calculations.^{28,29} Displacement parameters for Ba, Si, and Al have been refined anisotropically (except for the split position (Si,Al)(8a) and (Si,Al)(8b)). The parameters for Si and Al mixed on the same sites were constrained to be equal, and the atom ratio was fixed to the value given by the chemical analysis on all (Si,Al) sites, as lattice energy calculations (cf. Crystal Structure Description) based on the MAPLE concept (Madelung part of lattice energy)^{30,31} indicated no Si–Al ordering. The site occupancies of neighboring split positions (Ba(6a), Ba(6b); (Si,Al)(8a), (Si,Al)(8b); N(18a), N(18b); N(25a), N(25b)) were constrained to add up to 1. Details concerning the data collection and refinement are summarized in Table 1. Further details of the crystal structure investigation(s) may be obtained from Fachinformationszentrum Karlsruhe, 76344 Eggenstein-Leopoldshafen, Germany (fax, (+49)7247-808-666; e-mail, crysdata@fiz-karlsruhe.de, http://www.fiz-karlsruhe.de/request_for_deposited_data.html) by quoting the reference number CSD-419994.

- (10) Gál, Z. A.; Mallinson, P. M.; Orchard, H. J.; Clarke, S. J. *Inorg. Chem.* **2004**, *43*, 3998.
- (11) Huppertz, H.; Schnick, W. *Chem. Eur. J.* **1997**, *3*, 249.
- (12) Yamane, H.; DiSalvo, F. J. *J. Alloys. Compd.* **1996**, *240*, 33.
- (13) Ottinger, F. Ph. D. Thesis (Diss. ETH Nr. 15624), ETH Zürich, 2004.
- (14) Thompson, D. P. *Mater. Sci. Forum* **1989**, *47*, 21.
- (15) Watanabe, H.; Yamane, H.; Kijima, N. *J. Solid State Chem.* **2008**, *181*, 1848.
- (16) Ottinger, F.; Krosjakova, I.; Hametner, K.; Reusser, E.; Nesper, R.; Günther, D. *Anal. Bioanal. Chem.* **2005**, *383*, 489.
- (17) Grins, J.; Esmacilzadeh, S.; Shen, Z. *J. Am. Ceram. Soc.* **2003**, *86*, 727.
- (18) Pilet, G.; Grins, J.; Edén, M.; Esmacilzadeh, S. *Eur. J. Inorg. Chem.* **2006**, *18*, 3627.
- (19) Ischenko, V.; Kienle, L.; Jansen, M. *J. Mater. Sci.* **2002**, *37*, 5305.
- (20) Hecht, C.; Stadler, F.; Schmidt, P. J.; Schmedt auf der Günne, J.; Baumann, V.; Schnick, W. *Chem. Mater.* **2009**, *21*, in press.
- (21) Schmidt, P. J.; Mayr, W.; Meyer, J.; Schnick, W.; Hecht, C. S.; Stadler, F. PCT Int. Appl. WO2008096300, A1, 2008.
- (22) Mikami, M.; Uheda, K.; Kijima, N. *Phys. Status Solidi A* **2006**, *203*, 2705.
- (23) Piao, X.; Machida, K.; Horikawa, T.; Hanzawa, H.; Shimomura, Y.; Kijima, N. *Chem. Mater.* **2007**, *19*, 4592.
- (24) Uheda, K.; Hirotsaki, N.; Yamamoto, H. *Phys. Status Solidi A* **2006**, *203*, 2712.
- (25) Uheda, K.; Hirotsaki, N.; Yamamoto, Y.; Naito, A.; Nakajima, T.; Yamamoto, H. *Electrochem. Solid-State Lett.* **2006**, *9*, H22.
- (26) Schnick, W.; Huppertz, H.; Lauterbach, R. *J. Mater. Chem.* **1999**, *9*, 289.

- (27) Schlieper, T.; Milius, W.; Schnick, W. *Z. Anorg. Allg. Chem.* **1995**, *621*, 1380.
- (28) Sheldrick, G. M. *Acta Crystallogr., Sect. A* **2008**, *64*, 112.
- (29) Farrugia, L. J. *J. Appl. Crystallogr.* **1999**, *32*, 837.
- (30) Hoppe, R. *Angew. Chem.* **1966**, *78*, 52; *Angew. Chem., Int. Ed. Engl.* **1966**, *5*, 95.
- (31) Hoppe, R. *Angew. Chem.* **1970**, *82*, 7; *Angew. Chem., Int. Ed. Engl.* **1970**, *9*, 25.

Table 1. Crystal Data and Refinement Details of Ba₂AlSi₅N₉^a

formula	Ba ₂ AlSi ₅ N ₉
molar mass in g mol ⁻¹	568.20
crystal system	triclinic
space group	P1 (No. 1)
cell parameters in Å and deg	$a = 9.8600(10)$, $\alpha = 90.37(2)$ $b = 10.3200(10)$, $\beta = 118.43(2)$ $c = 10.3460(10)$, $\gamma = 103.69(2)$
cell volume in Å ³	890.7(3)
formula units per cell	4
X-ray density in g cm ⁻³	4.237
abs. coefficient in mm ⁻¹	9.545
$F(000)$	1032
crystal size in mm ³	0.17 × 0.12 × 0.09
diffractometer	STOE IPDS
radiation, monochromator	Mo K α ($\lambda = 0.71073$ Å), graphite
temperature in K	293(2)
2 θ range in deg	5.4–60.6
total no. of reflections	13615
independent reflections	5066
observed reflections	4651
absorption correction	numerical (X-RED 32; ⁵⁸ X-SHAPE ^{59,60})
refined parameters	449
GOF	0.984
R values [$I > 2\sigma(I)$]	$R1 = 0.0282$, $wR2 = 0.0678$
all data	$R1 = 0.0314$, $wR2 = 0.0686$
max/min residual electron density in e Å ⁻³	1.962/−1.726

^a Standard deviations are given in parentheses.

Table 2. Crystallographic Data of Ba₂AlSi₅N₉ Derived from Rietveld Refinement of X-ray Diffraction Data^a

formula	Ba ₂ AlSi ₅ N ₉
crystal system	triclinic
space group	P1 (No. 1)
lattice parameters in Å and deg	$a = 9.88129(10)$, $\alpha = 90.3507(7)$ $b = 10.32111(10)$, $\beta = 118.5685(6)$ $c = 10.36008(10)$, $\gamma = 103.6225(7)$
cell volume in Å ³	893.063(15)
formula units per cell	4
X-ray density in g cm ⁻³	4.226
$F(000)$	1032
structure refinement	Rietveld refinement, GSAS ³²
radiation	Cu K α_1 ($\lambda = 1.54056$ Å)
temperature in K	293(2)
profile range in deg	$5 \leq 2\theta \leq 90$
no. of data points	8500
observed reflections	1447
no. of refined parameters	265
no. of restraints	108
background function	shifted Chebyshev with 36 terms
profile function	pseudo-Voigt
R_p/wR_p	0.0237/0.0314
R_{int}^2	0.0537
GOF	1.59

^a An overall displacement parameter was used. Standard deviations are given in parentheses.

X-ray Powder Diffraction. X-ray powder diffraction data were collected on a STOE STADI P diffractometer (Cu K α_1 radiation, Ge(111) monochromator) in transmission geometry from a flat sample. For pattern fitting (LeBail algorithm) and Rietveld refinement, the GSAS program package³² was used. The result of the single-crystal X-ray diffraction data refinement was used as a starting model. The crystallographic data and details of the X-ray Rietveld refinement are given in Table 2. In Figure 1, both the observed and the calculated X-ray powder diffraction patterns for Ba₂AlSi₅N₉ and the corresponding difference profile for the Rietveld refinement are shown. The isotropic displacement parameters for all atoms were constrained to be equal, and the (Si,Al) site occupancies were fixed. Furthermore, all distances (Si,Al)–N

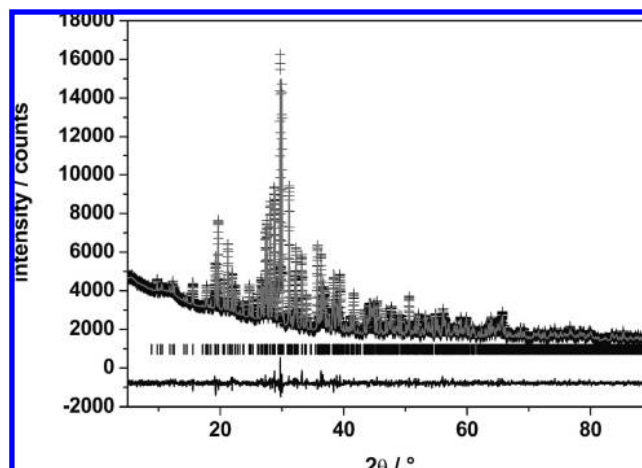


Figure 1. Observed (crosses) and calculated (line) X-ray powder diffraction patterns as well as difference profile for the Rietveld refinement of Ba₂AlSi₅N₉.

(including split positions) and a few distances N–N were restrained to the values, which were obtained in the single-crystal X-ray analysis, allowing for variations of 0.01 Å. The large number of atomic coordinates and the unsymmetrical lattice impeded a completely unconstrained refinement of all parameters; thus, distances and angles from the powder refinement will not be discussed but in general agree with those from the single crystal analysis. However, the Rietveld refinement of the X-ray diffraction data confirmed unequivocally the purity of the sample.

Neutron Powder Diffraction. Time-of-flight (TOF) neutron powder diffraction measurements have been carried out at the GEM diffractometer at ISIS (Rutherford Appleton Laboratory, Chilton, U.K.), which is well suited for diffraction measurements of small samples. About 100 mg of Ba₂AlSi₅N₉ were enclosed in a vanadium tube. For the refinement with GSAS,³² the back-scattering bank at $2\theta = 154.4^\circ$ has been used as it is characterized by good resolution and a large d -spacing range. Pronounced peak overlap impeded a detailed analysis; however, the structure model could well be confirmed. The starting model was again based on the single-crystal X-ray data. As the unsymmetrical lattice contains a large number of independent atom sites, a completely unrestrained refinement of the atomic coordinates was not possible. Therefore, most distances (Si,Al)–N were restrained to the values of the single-crystal analysis, allowing for variations of 0.01 Å.

As a result of the similar scattering lengths of Si and Al and the peak overlap mentioned above, these atoms could not be differentiated so that their ordering was not analyzed. In the final refinement, their site occupancies were fixed in the same way as for X-ray data, according to the results of the lattice energy calculations. The Rietveld profile fit for the structure model with the split sites is slightly better than for an idealized model. The sample did not contain any nitrogen-rich by-products like Si₃N₄, whose reflections cannot easily be detected in the background of X-ray powder diffractograms.³³

The structure refinement based on neutron data is summarized in Table 3. The observed and calculated neutron powder diffraction patterns for Ba₂AlSi₅N₉, as well as the corresponding difference profile of the Rietveld refinement, are shown in Figure 2.

Solid-State NMR. The NMR experiments were carried out on a BRUKER Avance DSX 500 spectrometer equipped with a commercial 4 mm MAS NMR probe. The magnetic field strength

(32) Larson, A. C.; Von Dreele, R. B. *GSAS - General Structure Analysis System*, Los Alamos National Laboratory: Los Alamos, NM, 1998.

(33) Kechele, J. A.; Oeckler, O.; Stadler, F.; Schnick, W. *Solid State Sci.* **2009**, *11*, 537.

Table 3. Crystallographic Data of Ba₂AlSi₅N₉ Derived from Rietveld Refinement of Neutron Diffraction Data^a

lattice parameters in Å and deg	$a = 9.8680(5)$, $\alpha = 90.352(2)$ $b = 10.3085(5)$, $\beta = 118.537(2)$ $c = 10.3552(6)$, $\gamma = 103.618(2)$
cell volume in Å ³	890.66(10)
detector position (2 θ) in deg	154.4
observed reflections	10862
no. of refined parameters	255
no. of restraints	105
temperature in K	293(2)
structure refinement	Rietveld refinement, GSAS ³²
background function	shifted Chebyshev with 20 terms
profile function	W. I. F. David (convolution of the Ikeda–Carpenter and pseudo-Voigt functions)
R _p /wR _p	0.0189/0.0232
R _{int} /2	0.0228
GOF	1.86

^a An overall displacement parameter was used. Standard deviations are in given in parentheses.

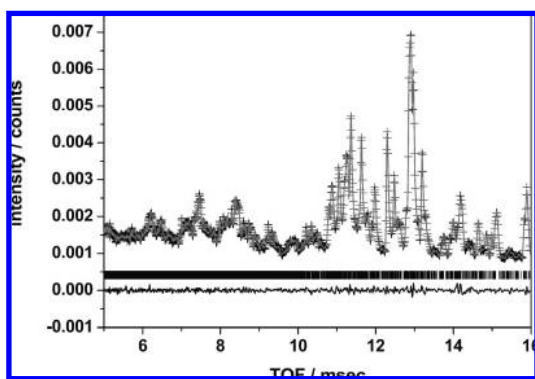


Figure 2. Observed (crosses) and calculated (line) neutron powder diffraction patterns as well as difference profile for the Rietveld refinement of Ba₂AlSi₅N₉.

was 11.75 T corresponding to ²⁹Si and ²⁷Al resonance frequencies of 99.5 and 130.5 MHz, respectively. The deshielding values reported for ²⁹Si and ²⁷Al refer to 1% Si(CH₃)₄ in CDCl₃ and a solution of Al(NO₃)₃ 1.1 mol kg⁻¹ in D₂O. The ¹H resonance of 1% Si(CH₃)₄ in CDCl₃ served as an external secondary reference using the Ξ values for ²⁹Si and ²⁷Al as reported by the IUPAC.³⁴ Saturation combs were applied prior to all repetition delays. The ²⁹Si spectrum was acquired with a repetition delay of 32 000 s (>3T₁) at a sample spinning frequency of 10 kHz. A triple-quantum ²⁷Al MQMAS 2D spectrum was acquired using a three-pulse sequence with a zero-quantum filter,³⁵ a repetition delay of 10 s, and rotor-synchronized sampling of the indirect dimension. Phase cycling involved the States method for acquisition of pure absorption line shapes and a 48 step phase cycle for coherence transfer pathway selection. The SOQE parameters and isotropic chemical shift values were determined by moment analysis^{35,36} from the extracted rows of the sheared MQMAS spectrum.

Thermogravimetric Investigations. The Thermogravimetric (TG) measurement has been performed in a thermoanalytical balance TGA 92-2400 (Setaram, Caluire, France), which was equipped with a measurement rod 92-2400-TG-ATG, 2400 °C, made of tungsten. A sample (62.3 mg) of Ba₂AlSi₅N₉ was heated in a tungsten crucible under He atmosphere to 1900 °C with a rate of 10 °C min⁻¹.

(34) Harris, R. K.; Becker, E. D.; Cabral de Menezes, S. M.; Granger, P.; Hoffman, R. E.; Zilm, K. W. *Pure Appl. Chem.* **2008**, *80*, 59.

(35) Amoureux, J.-P.; Fernandez, C.; Steuernagel, S. *J. Magn. Reson.* **1996**, *A123*, 116.

(36) Herreros, B.; Metz, A. W.; Harbison, G. S. *Solid State Nucl. Magn. Reson.* **2000**, *16*, 141.

Photoluminescence Measurements. The excitation and emission spectra in the range of 230–800 nm were recorded using a spectrofluorimeter (built at Philips Technologie GmbH, Forschungslaboratorien, Aachen)³⁷ equipped with a 150 W Xe lamp, two 500 mm Czerny–Turner monochromators, 1800 mm⁻¹ lattices, and 250/500 nm lamps. For recording of the reflection spectra a modified FS 920 system (Edinburgh Inst., Livingston, U.K.) was used.

Results and Discussion

Crystal Structure Description. Ba₂AlSi₅N₉ is a new type of framework silicate. The anionic framework is built up of (Si,Al)N₄ tetrahedra, which are connected by bridging N^[2] and N^[3] atoms. Neglecting less occupied alternative positions of split atoms, Figure 3b shows how the framework is built up of highly condensed silicate layers and both dreier and vierer rings³⁸ that interconnect the layers. The layers consist exclusively of vertex sharing (Si,Al)N₄ tetrahedra. Comparable highly condensed layers are known from layer silicates like MSi₂O₂N₂ (M = Ca, Sr, Ba, Eu)^{33,39–41} and also as partial structures in other frameworks like M₂Si₅N₈ (M = Ca, Sr, Ba).^{27,42} However, the up–down sequence of the tetrahedra in the layers of Ba₂AlSi₅N₉ (cf. Figure 3a) is unusual and has not been observed so far. The silicate layers are interconnected via dreier rings, which are built up of exclusively vertex-sharing tetrahedra. These rings are condensed via two shared corners to form pairs, building up one vierer ring per pair (cf. Figure 3c). The layers are further interconnected by a second kind of vierer rings built up of two vertex-sharing pairs of edge-sharing tetrahedra [T₂N₆] (cf. Figure 3c). Whereas [T₂N₆] entities are known from some nitridosilicates (e.g., BaSi₇N₁₀,¹¹ Ba₅Si₂N₆,¹² MSiN₂ (M = Sr, Ba)¹⁰) and some nitridoalumosilicates (e.g., Ca₅Si₂Al₂N₈, SrAlSi₄N₇),^{13,16,20} vierer ring formation by two pairs of edge-sharing tetrahedra has not been observed in silicates so far. However, the crystal structure of the nitridogallate Sr₃Ga₃N₅⁴³ contains an isoelectronic variant of such vierer rings.

There are different possibilities to distribute the Al and Si atoms to the tetrahedra centers of the framework. As a result of the smaller ion charge, Al³⁺ could be assumed to prefer the positions in the edge-sharing tetrahedra. The distances between tetrahedra centers of edge-sharing pairs are rather short so that the repulsion of the central ions is larger than in vertex-sharing tetrahedra pairs. Consequently, the Si⁴⁺ ions would be assumed in the tetrahedra centers of the layers and of the dreier rings. However, as both positions are in principle suitable for both Si and Al and disorder is

(37) Jüstel, T.; Krupa, J.-C.; Wiechert, D. U. *J. Lumin.* **2001**, *93*, 179.

(38) Liebau established the terms dreier, vierer, fünfer, and sechser rings. Thereby, a dreier ring can be described as a six-membered ring with three tetrahedral centres (e.g., Si) and three electronegative atoms (e.g., N), for example. The terms derive from the German numbers drei, vier, fünf, and sechs. Liebau, F. *Structural Chemistry of Silicates*; Springer: Berlin, 1985.

(39) Höpfe, H. A.; Stadler, F.; Oeckler, O.; Schnick, W. *Angew. Chem.* **2004**, *116*, 5656; *Angew. Chem., Int. Ed.* **2004**, *43*, 5540.

(40) Oeckler, O.; Stadler, F.; Rosenthal, T.; Schnick, W. *Solid State Sci.* **2007**, *9*, 205.

(41) Stadler, F.; Oeckler, O.; Höpfe, H. A.; Möller, M. H.; Pöttgen, R.; Mosel, B. D.; Schmidt, P.; Duppel, V.; Simon, A.; Schnick, W. *Chem. Eur. J.* **2006**, *12*, 6984.

(42) Schlieper, T.; Schnick, W. *Z. Anorg. Allg. Chem.* **1995**, *621*, 1037.

(43) Clarke, S. J.; DiSalvo, F. J. *Inorg. Chem.* **1997**, *36*, 1143.

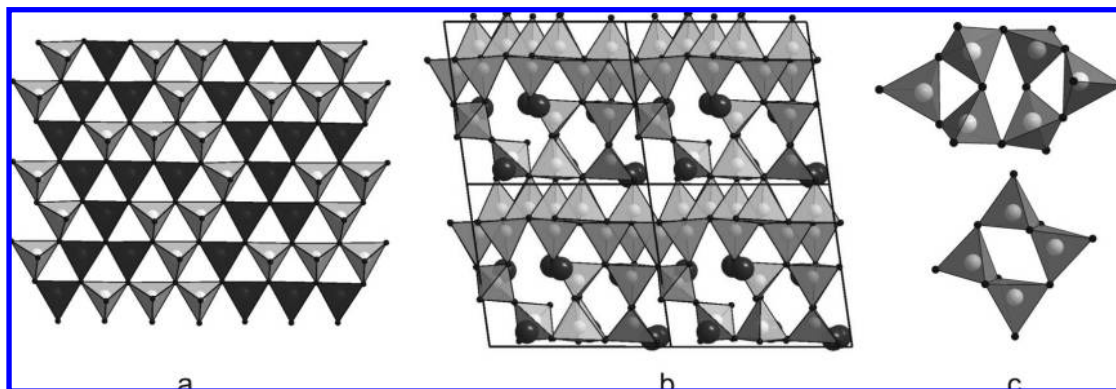


Figure 3. a: Highly condensed silicate layer of $\text{Ba}_2\text{AlSi}_5\text{N}_9$ (projection along $[0.8\ 0.2\ 1.2]$). For clarity, tetrahedra with vertices up are depicted light gray, those with vertices down dark gray (N black, Si/Al gray). b: Structure of $\text{Ba}_2\text{AlSi}_5\text{N}_9$, view along $[100]$. The $(\text{Si,Al})\text{N}_4$ tetrahedra are shown as well as the unit cell (Ba dark gray, Al/Si light gray, N black). c: Interconnecting dreier and vierer rings of $\text{Ba}_2\text{AlSi}_5\text{N}_9$ ((Si,Al) light gray, N black).

Table 4. Results of the MAPLE Calculations [kJ/mol] for Both Idealized $\text{Ba}_2\text{AlSi}_5\text{N}_9$ Structure Models^a

	Ba^{2+}	Al^{3+}	Si^{4+}	$\text{N}^{[2]3-}$	$\text{N}^{[3]3-}$	total MAPLE	Δ
model 1	1712–2004	6758–7548	8511–10391	3571–5481	4497–6690	107384	0.7%
model 2	1654–1932	8107–10092	4719–5393	5472–6198	107437	108194 kJ/mol	0.7%
total MAPLE ($\text{Ba}_2\text{Si}_5\text{N}_8 + \text{AlN}$): 108194 kJ/mol							
typical partial MAPLE values [kJ/mol]: Ba^{2+} , 1500–2000; Al^{3+} , 5500–6000; Si^{4+} , 9000–10200; $\text{N}^{[2]3-}$, 4600–6000; $\text{N}^{[3]3-}$, 5200–6300. ^{47,61}							

^a In model 1 (Si–Al ordering with Al in edge-sharing tetrahedra) the Si^{4+} and Al^{3+} ions are ordered; in model 2 the centers of the tetrahedra are statistically occupied with Si^{4+} and Al^{3+} ions, Δ = difference.

probably favored at high temperatures, the Al^{3+} and Si^{4+} ions may equally well be statistically distributed to all tetrahedra centers. Ordering at low temperatures would require a reconstructive mechanism and might thus be kinetically hindered. As both structure models could not be distinguished unequivocally both from X-ray and neutron diffraction data as a consequence of the similar atomic form factors of Al and Si, calculations of the lattice energy (MAPLE; Madelung part of lattice energy)^{30,31} were carried out. The results of these calculations are summarized in Table 4. Whereas the total MAPLE values for both models did not show significant differences, the partial MAPLE values differ significantly. In the ordered structure model, some values for $\text{N}^{[2]}$ are too small in comparison to reference values. Furthermore, the partial MAPLE values of some Si and $\text{N}^{[3]}$ are below the typical range, whereas for Al they are higher than typical values. For the disordered model, no unusual partial MAPLE value could be observed. According to our experience, this result favors a mixed occupancy of the tetrahedra centers.

Both ^{27}Al and ^{29}Si NMR resonances show broad non-resolved signals (cf. Figures 4 and 5), which are typical for disordered structures. The 2D ^{27}Al -MQMAS spectrum reveals that Al atoms with different quadrupole coupling tensors are present in the material (cf. Figure 4). The isotropic chemical shift values which can be determined from the ^{27}Al -MQMAS spectrum are all larger than 110 ppm. For four-fold coordinated Al atoms literature values⁴⁴ indicate that the observed values can only be explained by AlN_4 but not by $\text{AlN}_{4-x}\text{O}_x$ tetrahedra (with $1 \leq x \leq 4$). Since we would expect the ^{27}Al -MQMAS experiment to resolve four Al sites in the ordered model, we conclude that ^{27}Al NMR gives support for the disordered model. The ^{29}Si NMR spectrum

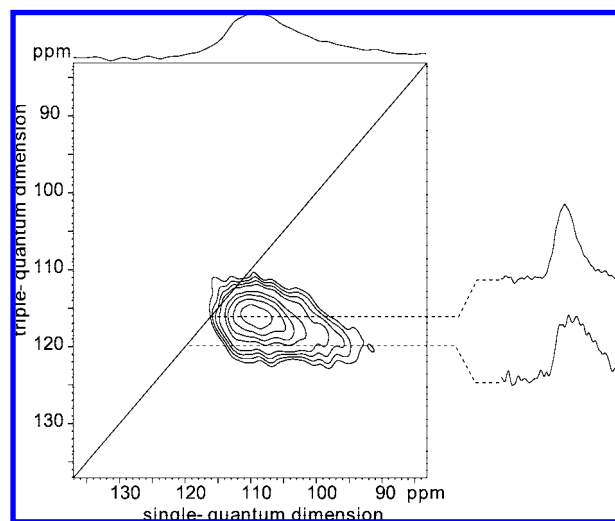


Figure 4. Sheared ^{27}Al 2D MQMAS NMR spectrum of $\text{Ba}_2\text{AlSi}_5\text{N}_9$; rows have been extracted at the indicated positions and analyzed for the isotropic chemical shift δ_{iso} and the SOQE parameter ($\delta_{\text{iso}} = 112.6$ and 113.5 ppm, SOQE = 4.0 and 5.6 MHz for the upper and lower row, respectively).

is less conclusive since the observed isotropic chemical shift range of about -43 to -58 ppm overlaps with known values for ^{29}Si in SiN_4 , SiN_3O , and SiN_2O_2 tetrahedra.^{36,45} The latter, SiN_2O_2 , can only be excluded because then also $\text{AlN}_{4-x}\text{O}_x$ (with $x > 0$) would have to be present.

Bond lengths (Si,Al)–N depend on both the coordination of N atoms and the linkedness of the tetrahedra. In vertex-sharing tetrahedra, the distances (Si,Al)– $\text{N}^{[2]}$ (1.633–1.739 Å) are in the typical range for Si– $\text{N}^{[2]}$ in nitridosilicates ($\text{BaSi}_7\text{N}_{10}$ 1.64–1.69 Å;¹¹ $\text{Ba}_2\text{Si}_5\text{N}_8$ 1.66–1.71 Å;²⁷ $\text{Ba}_2\text{Nd}_7\text{Si}_{11}\text{N}_{23}$ 1.67–1.755 Å)⁴⁶ and slightly shorter than (Si,Al)– $\text{N}^{[2]}$ bonds in CaSiAlN_3 (1.790 Å).¹³ The distances

(44) Mackenzie, K. J. D.; Smith, M. E. *Multinuclear Solid-State NMR of Inorganic Solids*; Pergamon: Amsterdam, 2002.

(45) Kempgens, P.; Harris, R. K.; Yu, Z.; Thompson, D. P. *J. Mater. Chem.* **2001**, *11*, 2507.

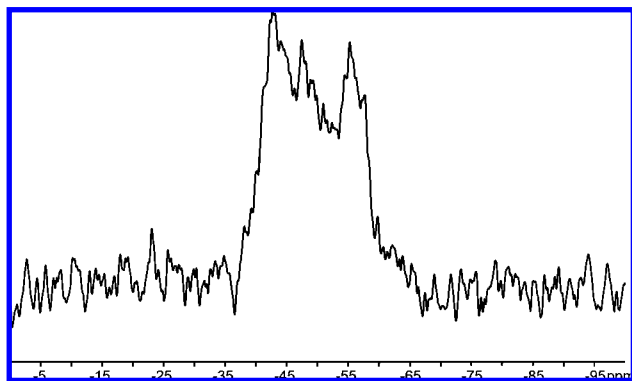


Figure 5. ²⁹Si solid-state NMR with several unresolved signals in the range of about -43 to -58 ppm.

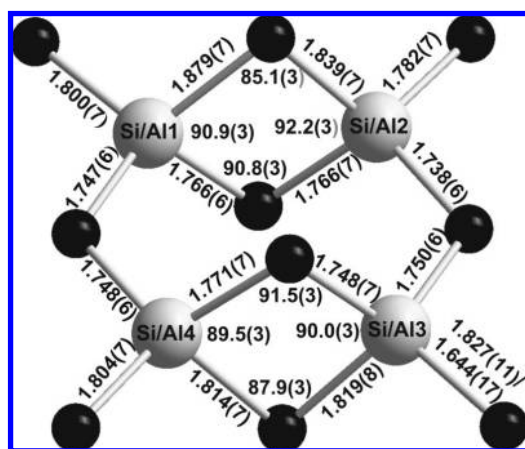


Figure 6. Interatomic distances and bond angles within the edge-sharing vierer rings. Standard deviations are given in parentheses.

(Si,Al)–N^[3] range over a large interval (1.706–1.886 Å), the long distances involving either the rather imprecise split positions (Si,Al)(8a) and (Si,Al)(8b) or N^[3] atoms that bridge the highly condensed silicate layers with interconnecting both dreier and edge-sharing vierer rings. All other distances (Si,Al)–N^[3] are in the typical range for Si–N^[3] (BaSi₇N₁₀ 1.69–1.79 Å,¹¹ Ba₂Si₅N₈ 1.74–1.79 Å)²⁷ and (Si,Al)–N^[3] in CaSiAlN₃ (1.807–1.832 Å).¹³

The N–(Si,Al)–N bond angles are between 90.1 and 128.7°. Large deviations from the ideal angle for tetrahedra (109°) could only be observed for the Si or N split positions. All other values are close to the regular tetrahedral angle (102.0–117.1°). In the case of the angles (Si,Al)–N^[2]–(Si,Al) (105.4–130.1°) and (Si,Al)–N^[3]–(Si,Al) (86.5–131.4°), split positions also account for the highest and lowest values. Neglecting these values, the angles Si–N^[3]–Si in BaSi₇N₁₀ are approximately in the same range (109.9–132.9°),¹¹ and the reported range for the Si–N^[2]–Si angles in Ba₂Nd₇Si₁₁N₂₃ is even larger (117.9–180°).⁴⁶ The angle at N(22)^[2] of about 112° in the framework of Ba₂AlSi₅N₉ is the smallest one, disregarding the split positions, and is in the same range as the Si–N^[2]–Si bond angles in Sr₃Ln₁₀Si₁₈Al₁₂O₁₈N₃₆ (Ln = Ce (112.2°); Pr (111.8°); Nd (111.6°)).⁴⁷ However, the edge-sharing tetrahedra were not regarded in this discussion.

Within the pairs of edge-sharing tetrahedra (cf. Figure 6), the bond lengths (Si,Al)–N are between 1.644 and 1.879 Å, which is similar to the comparable distances in BaSi₇N₁₀

(1.64–1.77 Å),¹¹ Ba₅Si₂N₆ (1.74–1.84 Å),¹² and Ca₅Si₂Al₂N₈ ([Si₂N₆]¹⁰⁻, 1.725–1.860 Å; [Al₂N₆]¹²⁻, 1.833–1.952 Å).^{13,16} The angles (Si,Al)–N–(Si,Al) (85.1–91.5°) and N–(Si,Al)–N (89.5–92.2°) are also comparable to the angles in other nitrido(alumo)silicates with edge-sharing tetrahedra (BaSi₇N₁₀ Si–N–Si 90.2 and 91.2°, N–Si–N 89.3°;¹¹ Ba₅Si₂N₆ Si–N–Si 88.5 and 89.4°, N–Si–N 90.7 and 91.4°;¹² Ca₅Si₂Al₂N₈ Si–N–Si 86.4°, Al–N–Al 89.1°, N–Si–N 93.6°, N–Al–N 90.7°).^{13,16} The distances between the centers of the edge-sharing tetrahedra (2.515 and 2.520 Å) are also in the typical range (BaSi₇N₁₀ 2.506 Å;¹¹ Ba₅Si₂N₆ 2.556 Å;¹² Ca₅Si₂Al₂N₈ 2.450 Å (Si–Si), 2.708 Å (Al–Al)).^{13,16}

The framework of Ba₂AlSi₅N₉ hosts eight crystallographically independent Ba²⁺ ions with coordination numbers between 6 and 10, which are shown in Figure 7. The distances of Ba–N are between 2.547 and 3.680 Å. Accordingly, these are shorter than the smallest sum of the ionic radii (2.81 Å;⁴⁸ 2.90 Å⁴⁹), but the distances are slightly shorter than in well known barium nitridosilicates (e.g., Ba₂Si₅N₈ 2.68–3.00 Å;²⁷ Ba₅Si₂N₆ 2.61–3.40 Å;¹² BaSi₇N₁₀ 2.91–3.53 Å)¹¹ and comparable with the short distances Ba–N in Ba₂VN₃ (2.50–3.16 Å)⁵⁰ or Ba₁₀[Ti₄N₁₂] (2.56–3.59 Å).⁵¹

In Figure 7, the slightly different, but very similar coordination spheres of both sites of the split position Ba(6a)/Ba(6b) are depicted. These two alternative Ba sites correlate with an alternative position of tetrahedra. Ba(6b) is too close to (Si,Al)(8a), which is replaced by (Si,Al)(8b) if Ba(6b) is present. Consequently, two nitrogen sites (N(18), N(25)) also require splitting. When (Si,Al)(8b)₄ tetrahedra are present, they are connected by a common corner with the tetrahedra around (Si,Al)(6).

Thermogravimetric Investigation. The TG measurement (cf. Figure 8) shows that Ba₂AlSi₅N₉ is stable up to about 1515 °C under He atmosphere. Above this temperature, the compound decomposes rapidly under formation of gaseous products. This result is similar to thermal analyses of other nitridosilicates, as, for example, the thermolysis of Ba₄Sm₇[Si₁₂N₂₃O][BN₃] starts at about 1410 °C.^{8,52} The thermal stability of Ba₂AlSi₅N₉ observed in the TG measurement is reduced in comparison to the temperature for the synthesis of this compound. This effect is probably due to the use of He instead of N₂. Furthermore, Ba₂AlSi₅N₉ also starts to decompose under N₂ atmosphere during the synthesis, if a long time for annealing is chosen at the maximum temperature.

Luminescence. For the investigation of photoluminescence, samples of Ba₂AlSi₅N₉ were doped with 2 mol % Eu²⁺. Under daylight, the obtained crystals are colored light orange as a consequence of the 4f⁷(⁸S_{7/2}) → 4f⁶5d absorption

(46) Huppertz, H.; Schnick, W. *Angew. Chem.* **1997**, *109*, 2765; *Angew. Chem., Int. Ed. Engl.* **1997**, *36*, 2651.

(47) Lauterbach, R.; Irran, E.; Henry, P. F.; Weller, M. T.; Schnick, W. *J. Mater. Chem.* **2000**, *10*, 1357.

(48) Shannon, R. D. *Acta Crystallogr., Sect. A* **1976**, *32*, 751.

(49) Baur, W. H. *Crystallogr. Rev.* **1987**, *1*, 59.

(50) Gregory, D. H.; Barker, M. G.; Edwards, P. P.; Siddons, D. J. *Inorg. Chem.* **1995**, *34*, 3912.

(51) Seeger, O.; Strähle, J. Z. *Anorg. Allg. Chem.* **1995**, *621*, 761.

(52) Orth, M.; Hoffmann, R.-D.; Pöttgen, R.; Schnick, W. *Chem. Eur. J.* **2001**, *7*, 2791.

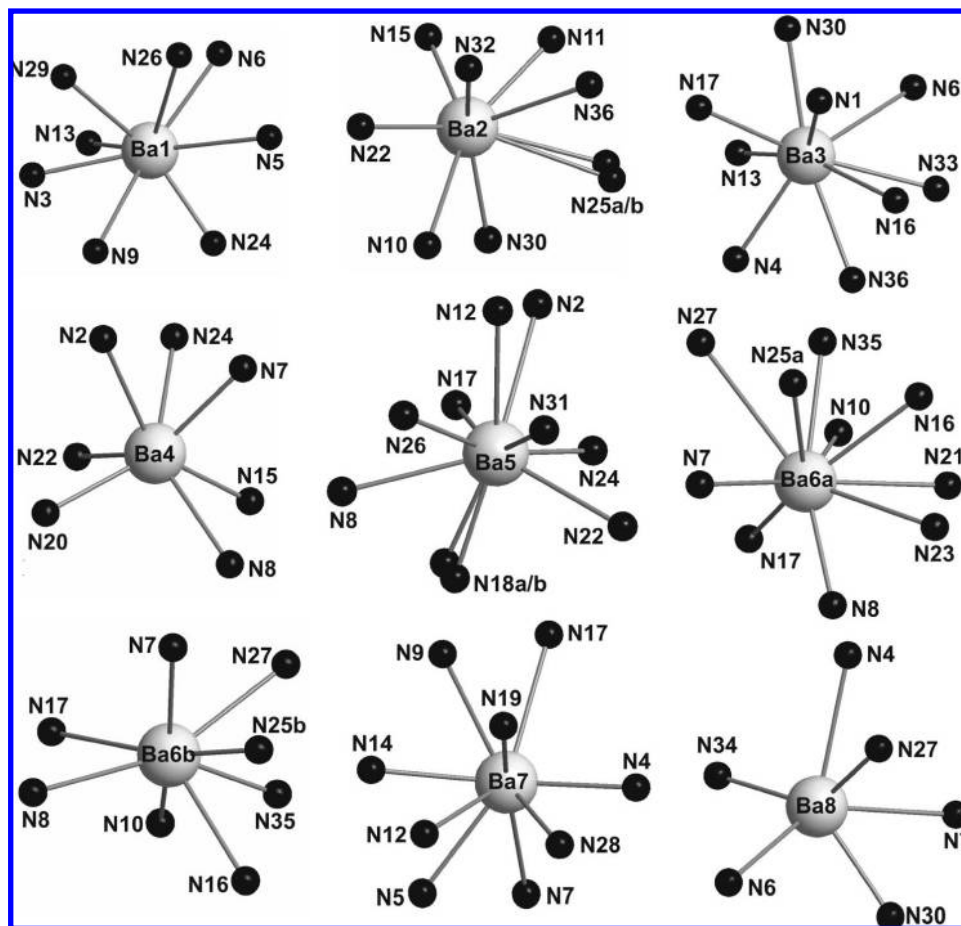


Figure 7. Coordination spheres of Ba^{2+} in $\text{Ba}_2\text{AlSi}_5\text{N}_9$ (Ba light gray, N black).

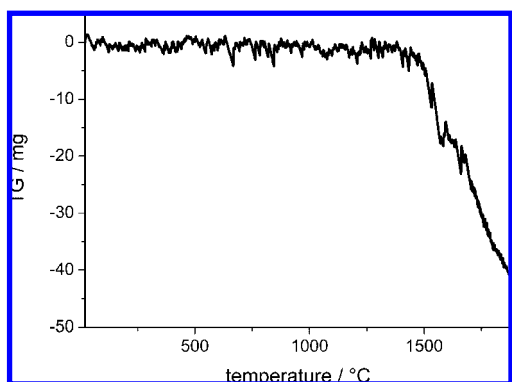


Figure 8. TG heating curve of $\text{Ba}_2\text{AlSi}_5\text{N}_9$ recorded between RT and 1900 °C with a heating rate of 10 °C min^{-1} . The weight of the sample was 62.3 mg.

of Eu^{2+} in the blue to green spectral range. The excitation, emission, and reflection spectra of $\text{Ba}_{1.96}\text{AlSi}_5\text{N}_9:\text{Eu}_{0.04}$ are shown in Figure 9. For 450 nm excitation, a broadband emission spectrum peaking at 584 nm is obtained that shows a spectral width (FWHM) of ~ 100 nm. Similar luminescence characteristics were found for yellow emitting $\text{Ba}_2\text{Si}_5\text{N}_8:\text{Eu}$ that shows an emission maximum in the same spectral range (~ 580 nm for 2 mol % Eu^{2+} , FWHM ~ 90 nm).^{1,53–57} $\text{CaAlSiN}_3:\text{Eu}$, one of the first described Eu^{2+} doped nitridoalumosilicate phosphors, shows an emission band peaking at 650 nm (FWHM ~ 90 nm).^{23–25} The red shift of the emission of $\text{CaAlSiN}_3:\text{Eu}$ compared to $\text{Ba}_2\text{AlSi}_5\text{N}_9:\text{Eu}$ may be explained by the stronger N ligand field in the Ca

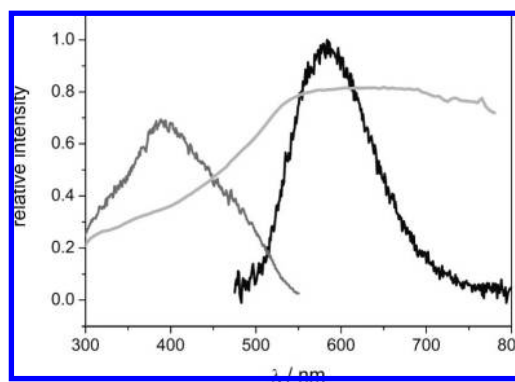


Figure 9. Excitation (dark gray), emission (black, 450 nm excitation), and reflection spectra (light gray) of $\text{Ba}_2\text{AlSi}_5\text{N}_9$.

compound that leads to a lowering of the energy separation between the Eu^{2+} 4f and 5d states and thus to a shift of absorption and emission bands toward lower energies.

The larger band width of the Eu^{2+} emission in $\text{Ba}_2\text{AlSi}_5\text{N}_9$ compared to yellow emitting $\text{Ba}_2\text{Si}_5\text{N}_8:\text{Eu}$ and red emitting $\text{CaSiAlN}_3:\text{Eu}$ is most likely caused by the different number of crystallographically independent cation sites that may be populated with Eu^{2+} . While there is only one Ca^{2+} site in CaSiAlN_3 ¹³ and two Ba^{2+} sites in $\text{Ba}_2\text{Si}_5\text{N}_8$,²⁷ the framework of $\text{Ba}_2\text{AlSi}_5\text{N}_9$ hosts eight crystallographically independent Ba^{2+} ions that differ significantly in coordination (CN = 6–10); thus, a composed Eu^{2+} emission band originating from various sites can be expected.

The luminescence quantum efficiency of $Ba_{1.96}AlSi_5N_9:Eu_{0.04}$ has been determined to be relatively low (22.3 %) compared with that of other red phosphors (e. g. $Ba_2Si_5N_8$ or $CaAlSiN_3$). However, within this investigation we have not optimized the samples concerning this matter.

Conclusion

With the synthesis of $Ba_2AlSi_5N_9$, the first compound in the system Ba–Si–Al–N could be obtained. This novel nitridoalumosilicate is characterized by its unusual silicate framework, which contains not only vertex-sharing tetrahedra but also edge-sharing tetrahedra. This framework is built up of highly condensed silicate layers, which are interconnected

by different kinds of rings. In this anionic substructure eight Ba^{2+} ions are situated with coordination numbers between 6 and 10. $Ba_2AlSi_5N_9$ is one of the first nitridoalumosilicates whose luminescence properties were investigated. As a result of the good thermal stability and the fact that an oxygen concentration could be almost excluded, the nitridoalumosilicates are suited as red rare earth-doped phosphors for white light LEDs. For an optimization of the luminescence properties, compounds with a higher symmetry could be valuable. In this context, $Ba_2AlSi_5N_9$ could trigger as initiation for a further systematic investigation of Ba containing nitridoalumosilicates.

Acknowledgment. The authors thank Dr. Stefanie Jakob and Thomas Miller for the collection of the single-crystal data, as well as Andreas Sattler for performing the DTA/TG measurement. Solid-state NMR measurements by Christian Minke as well as EELS analysis by Dr. Markus Döblinger are gratefully acknowledged. Furthermore, we thank Dr. Winfried Kockelmann for his assistance during the neutron measurements at the GEM diffractometer at ISIS/Rutherford Appleton Laboratory. This work was financially supported by the Fonds der Chemischen Industrie.

Supporting Information Available: The atomic coordinates, (equivalent) isotropic and anisotropic displacement parameter, and site occupancy factors of $Ba_2AlSi_5N_9$ as well as selected bond length and angles. This material is available free of charge via the Internet at <http://pubs.acs.org>.

CM803233D

-
- (53) Schmidt, P.; Tuecks, A.; Meyer, J.; Bechtel, H.; Wiechert, D.; Mueller-Mach, R.; Mueller, G.; Schnick, W. *Proceedings of SPIE-The International Society for Optical Engineering* **2007**, 6669, 66690P/1.
 - (54) Piao, X.; Machida, K.; Horikawa, T.; Hanzawa, H. *Appl. Phys. Lett* **2007**, 91, 041908/1.
 - (55) Li, Y. Q.; vanSteen, J. E. J.; van Kreveld, J. W. H.; Botty, G.; Delsing, A. C. A.; DiSalvo, F. J.; deWith, G.; Hintzen, H. T. *J. Alloys Compd.* **2006**, 417, 273.
 - (56) Mueller-Mach, R.; Mueller, G. O.; Schmidt, P. J.; Wiechert, D. U.; Meyer, J. *Proceedings of SPIE-The International Society for Optical Engineering* **2005**, 5941, 59410Z/1.
 - (57) Höpfe, H. A.; Lutz, H.; Morys, P.; Schnick, W.; Seilmeier, A. *J. Phys. Chem. Solids* **2000**, 61, 2001.
 - (58) *X-Red 32*, Version 1.31; STOE and Cie GmbH: Darmstadt, 2005.
 - (59) *X-SHAPE*, Version 2.07; STOE and Cie GmbH: Darmstadt, 2005.
 - (60) Herrendorf, W.; Bärnighausen, H. *HABITUS -Program for Numerical Absorption Correction*; Universitäten Karlsruhe/Giessen, 1993/1997.
 - (61) Höpfe, H. A.; Dissertation, Ludwig-Maximilians-Universität München, 2003.